CrossMark

Potential impacts of emissions associated with unconventional hydrocarbon extraction on UK air quality and human health

A. T. Archibald [1,2] ⬤ · C. Ordóñez [3,4] · E. Brent [1] · M. L. Williams [5]

Abstract

Here, we report the first results of model sensitivity simulations to assess the potential impacts of emissions related to future activities linked to unconventional hydrocarbon extraction (fracking) in the UK on air pollution and human health. These simulations were performed with the Met Office Air Quality in the Unified Model, a new air quality-forecasting model, and included a wide range of extra emissions of volatile organic compounds (VOCs) and nitrogen oxides (NO_x) to reflect emissions from the full life cycle of fracking-related activities and simulate the impacts of these compounds on levels of nitrogen dioxide (NO_2) and ozone (O_3). These model simulations highlight that increases in NO_x and VOC emissions associated with unconventional hydrocarbon extraction could lead to large local increases in the monthly means of daily 1-h maximum NO_2 of up to + 30 ppb and decreases in the maximum daily 8-h mean O_3 up to − 6 ppb in the summertime. Broadly speaking, our simulations indicate increases in both of these compounds across the UK air shed throughout the year. Changes in the 1-h maximum of NO_2 and 8-h mean of O_3 are particularly important for their human health impacts. These respective changes in NO_2 and O_3 would contribute to approximately 110 (range 50–530) extra premature-deaths a year across the UK based on the use of recently reported concentration response functions for changes in annual average NO_2 and O_3 exposure. As such, we conclude that the release of emissions of VOCs and NO_x be highly controlled to prevent deleterious health impacts.

Keywords Fracking · UK air pollution · Unconventional hydrocarbons · Ozone · Nitrogen dioxide

Introduction

Hydraulic fracturing or 'fracking' describes the industrial process used to extract hydrocarbons by pervasively fracturing a shale unit (termed shale plays) with high-pressure water, mixed with sand and chemical additives (Bickle 2012).

This source of unconventional hydrocarbons has created a large amount of interest from investors in the petroleum industry as well as environmentalists and the general public concerned with the impacts associated with it. Whilst fracking as a technique has a long history, its wide-scale uptake is much more recent. This increased uptake is driven largely by technological breakthroughs such as horizontal drilling, which will ultimately allow those involved to extract more of the oil and gas from geological reservoirs than previous methods would have permitted. In the USA, natural gas (an industry term for gaseous mixtures of hydrocarbons rich in methane) from shale accounted for only ~ 2% of total production in 2004. Owing to proliferation in the fracking of shale plays, by 2035, shale gas is predicted to account for over 63% of total production (BP 2014). This exploitation of shale oil and gas coincides with the USA becoming the world's largest producer of natural gas. In the USA, shale fracking sites are generally found in large geological basins, for example in the Rocky and Appalachian Mountains and Great Plains. Generally speaking, the most productive sites are in very rural areas well away from large population settlements (US Energy Information Administration 2015).

Whilst methane is one of the most important hydrocarbons extracted from fracking, there are a large number of

✉ A. T. Archibald
ata27@cam.ac.uk

1   Department of Chemistry, University of Cambridge, Cambridge CB2 1EW, UK

2   NCAS-Climate, University of Cambridge, Cambridge, UK

3   Met Office, FitzRoy Road, Exeter EX1 3PB, UK

4   Dpto. de Física de la Tierra y Astrofísica, Facultad de Ciencias Físicas, Universidad Complutense de Madrid, 28040 Madrid, Spain

5   Environmental Research Group, Kings College London, London, UK

Springer

non-methane volatile organic compounds (NMVOCs) held within the shale plays, including alkanes, cycloalkanes, aromatic compounds and bicyclic hydrocarbons (Sommariva et al. 2014).

The potential environmental and health impacts associated with fracking are varied in terms of their sources and mechanisms of action (Adgate et al. 2014). Of particular interest is the influence of fracking on air quality. The compositions of the emissions associated with fracking are dependent on the particular phase in the life cycle of the fracking well (Moore et al. 2014). However, significant emissions of nitrogen oxides (NO_x) and NMVOCs (also referred to as VOCs) are common throughout this life cycle. Both NO_x and NMVOCs represent important species in the production of ozone (O_3), a secondary pollutant associated with adverse health effects (Brunekreef and Holgate 2002). Elevated levels of O_3, especially in urban areas, are of particular concern in the USA, where fracking has been adopted on a large scale. As such, much of the literature concerned with air pollution resulting from fracking focuses on the relationship between NO_x and NMVOC emissions and O_3 concentrations (e.g. Edwards et al. 2014 and references therein) and these interactions provide an interesting point of comparison for an assessment of the potential atmospheric impacts of fracking in the UK.

Fracking in the UK remains a controversial issue. However, the House of Commons' rejection of a moratorium in January 2014 means that wide-scale adoption of fracking is a significant possibility. Whilst there has been considerable speculation about the environmental impacts of fracking in the UK (Environmental Audit Committee 2015) mainly based on extrapolation from the USA, there have been no studies investigating the impacts of any potential risks. It is, therefore, important to provide some detail of how the consequences of fracking in the UK may differ from those of the USA. This sort of preparatory investigation may also provide vital information for the development of effective, evidence-based regulation.

The aim of this study is to determine how increased emissions of VOCs and NO_x in regions where fracking could take place in the UK may impact air quality and ultimately human health. To achieve this, we make use of a recently developed numerical air quality-forecasting model, Air Quality in the Unified Model (AQUM) (Savage et al. 2013). The 'The AQUM model' section provides a description of the AQUM model set-up used in this study. The 'Emission scenarios' section provides information on our emission scenarios for increases in VOCs and NO_x in the potential fracking regions, whilst in the 'Results' section, we present the results obtained from our AQUM simulations, including analyses of comparisons with observations of O_3 and NO_2 from the UK Automatic Urban and Rural Network (AURN) and the results from our emission scenarios. In the sections 'Results' and 'Discussion', we discuss and conclude the study and make recommendations for further work.

The AQUM model

AQUM is a limited area configuration of the Met Office Unified Model (UM), used operationally to provide a 5-day air quality forecast for the UK (Savage et al. 2013). The model is operated with a 12-km × 12-km horizontal resolution grid covering part of Western Europe and 38 vertical levels spanning from the ground up to around 40 km altitude. The representation of chemistry in AQUM is given by the regional air quality (RAQ) chemistry scheme of the United Kingdom Chemistry and Aerosols (UKCA) sub-model of the UM, whilst aerosol processes are parameterised within the Coupled Large-Scale Aerosol Simulator for Studies in Climate (CLASSIC) sub-model.

The RAQ chemistry mechanism includes 40 transported species and 18 non-advected species, 116 gas-phase reactions and 23 photolytic reactions. It takes account of emissions for NO_x, carbon monoxide (CO) and the following NMVOC species: ethane (C_2H_6), propane (C_3H_8), butane (C_4H_{10}), ethene (C_2H_4), propene (C_3H_6), formaldehyde (HCHO), acetaldehyde (CH_3CHO), acetone (CH_3COCH_3), methanol (CH_3OH), isoprene (C_5H_8), toluene and o-xylene. Removal by wet and dry deposition is considered for 19 and 16 species, respectively. CLASSIC is a bulk aerosol scheme, where the following aerosol species are treated as an external mixture: ammonium sulphate [$(NH_4)_2SO_4$], ammonium nitrate (NH_4NO_3), black carbon (BC), fossil fuel organic carbon (FFOC), biomass burning aerosol, mineral dust, sea salt aerosol and a climatology of biogenic secondary organic aerosol (BSOA). The model has two-way coupling of oxidants between the aerosol and gas-phase chemistry schemes. Within CLASSIC, sulphur dioxide (SO_2) and dimethyl sulphide (DMS) are emitted and oxidised into aerosol sulphate (SO_4^{2-}) by four oxidants whose concentrations are calculated in RAQ: O_3, hydroxyl radical (OH), hydroperoxyl radical (HO_2) and hydrogen peroxide (H_2O_2). The reaction of sulphate with ammonia (NH_3) produces ammonium sulphate. Any excess ammonia reacts with nitric acid (HNO_3), provided by RAQ, to form ammonium nitrate. Finally, the depleted oxidant concentrations are passed back to the RAQ chemistry scheme of UKCA. (For further details on CLASSIC, see Appendix A of Bellouin et al. (2011).) A full description of the RAQ chemistry scheme and the AQUM modelling system is provided by Savage et al. (2013).

Lateral boundary conditions (LBCs) for meteorological fields are provided by the operational forecast of the Met Office global model. LBCs for chemistry and aerosols are derived from the operational forecast of the Monitoring Atmospheric Composition and Climate (MACC) global model (Flemming et al. 2009).

The main difference between the model configuration presented by Savage et al. (2013) and the one used in this study is the treatment of anthropogenic gas-phase emissions within

UKCA. In the present study, monthly emission fields used in the AQUM control run are created for the year 2012 by merging data from three emission inventories: the National Atmospheric Emissions Inventory (NAEI) at 1-km resolution over the UK (Passant et al. 2014), ENTEC shipping data around the UK at 5 km (Whall et al. 2010) and the MACC-II regional emission inventory at 0.125° longitude × 0.0625° latitude resolution (Kuenen et al. 2014) for the rest of the domain. The ENTEC and MACC emission data used here were compiled for 2007 and 2009, respectively, but they are scaled according to published totals from the European Monitoring and Evaluation Programme (EMEP) for 2012. Data from all three sources are interpolated to the AQUM 12-km grid prior to merging. In the version of AQUM introduced by Savage et al. (2013), anthropogenic monthly emission fields for gas-phase species were spread equally over the first four model layers (20, 80, 180 and 320 m mid-altitude) and hourly emission factors derived from an analysis of traffic cycles were applied. This simplistic approach has been replaced here by a more comprehensive system that enables the separate treatment of emission fields according the so-called selected nomenclature for air pollutants (SNAP) source sectors. In particular, the vertical disaggregation of emissions consists of separate vertical profiles for each SNAP sector based on calculations performed with the SMOKE-EU plume rise model (Bieser et al. 2011). Emissions in our simulations are initially redistributed in the vertical among the EMEP vertical layers (Simpson et al. 2012) following the Bieser et al. (2011) recommendations, but adding a supplementary 0–20-m layer as done by Mailler et al. (2013) to account for the fact that the first EMEP layer is relatively thick (92 m). The resulting matrix attributing emissions to vertical layers is equivalent to that of Mailler et al. (2013), but interpolated to the AQUM vertical grid. Hourly and daily emission factors based on those created by TNO for the MACC project (Denier van der Gon et al. 2011) are also applied to account for the diurnal and weekly cycles of each SNAP source sector.

The use of a comprehensive treatment of gas-phase emissions has a moderate impact on the modelled near-surface concentrations of pollutants. Basically, the new vertical disaggregation of emissions results in somewhat higher effective emission heights compared to a previous configuration which resembles that of Savage et al. (2013). This yields some decreases in the peak NO_x concentrations at the surface and consequently a reduction in the number of events with very low O_3 concentrations. The combined effect of the new vertical and temporal profiles of emissions also results in improved diurnal cycles for both NO_x and O_3 when compared to near-surface observations from the UK Automatic Urban and Rural Network (AURN). However, this does not remove all biases from the model.

Emission scenarios

A number of model simulations, summarised in Table 1, have been conducted to simulate the year 2013 and perform an annual assessment of the impact of emissions related with fracking on air quality over the UK.

The location/extent of the additional emissions was constrained by the locations of shale prospective areas for fracking in the UK identified by the British Geological Survey (Fig. 1). These include (i) the Jurassic Weald Basin in the South East of England (Andrews 2014), (ii) the Carboniferous Bowland-Hodder Shale in the North of England (Andrews 2013) and (iii) the Carboniferous Midland Valley of Scotland (Monaghan 2014). These areas already contain licenced blocks, granted by the Department for Energy and Climate Change (DECC), for the exploration and extraction of oil and gas. Only emissions in the AQUM grid cells that were within these licenced blocks were modified.

It is critical to note that as there are no wide-scale fracking plants in operation in the UK at present, the scenarios we have explored with AQUM test the sensitivity of air pollution to potential changes in emissions. Fracking wells themselves are not likely to be allowed (by law) to become major sources of VOC emissions in the UK. The DECC and other government agencies have acknowledged that the major risk to air pollution is in the associated surface-based activities that rely on heavy-duty internal combustion engines (particularly diesel fuelled engines which are known to have significant impacts on human health (IARC 2012)). As such, we took the grid square in the UK AQUM emission data sets (see the 'The AQUM model' section for details of the sources of emissions data) with the highest emissions of VOC and NO_x from SNAP sector 5 (extraction and distribution of fossil fuels and geothermal energy) or SNAP sector 7 (road transport) for 2012 as a starting point under the premise that additional emissions from fracking-related activity could potentially mirror the current UK emission situation. These emissions were then added to each of the grid squares in the model where shale gas extraction licences have been granted (Fig. 1) to create scenario 1 (Table 1). The NO_x and VOC emissions were then further increased through scenarios 2–4 to span a wide range of potential increases in VOC and NO_x emissions (following Edwards et al. (2014)) to determine more about the role of NO_x limitation and VOC limitation on potential O_3 increases (Sillman 1999). These increments to the emissions in AQUM have been added to SNAP sector 5 and have the appropriate temporal and vertical profiling applied (see the 'The AQUM model' section).

An important question to ask is whether or not these emission scenarios are realistic. Given the uncertainty present, it is impossible to answer this with a yes or a no. Our aim is to span plausible to potential worst-case scenarios (outline in Table 1).

Table 1 Summary of the AQUM simulations conducted for 2013 to assess the impact of emissions from hydraulic fracturing including the modifications to total VOC and NO_x emissions

| Simulation	Notes	$\Delta VOC^{\ddagger}$ Tg/year (%)	ΔNO_x Tg/year (%)
Control	Control run without fracking emissions	–	–
Scenario 1	Additional emissions of NO_x and VOCs from fracking	0.13 (25%)	0.04 (4.9%)
Scenario 2	Like 'scenario 1' but with higher NO_x and VOC emissions	0.27 (51%)	0.17 (19.6%)
Scenario 3	Like 'scenario 1' but with higher VOC emissions	0.27 (51%)	0.04 (4.9%)
Scenario 4	Like 'scenario 3' but with higher VOC emissions	0.55 (104%)	0.04 (19.6)

‡ The VOC emissions into the model include the full suite of emissions discussed in the 'The AQUM model' section

Vengosh et al. (2017) analysed over 100 papers published since 2013 on the topic of unconventional hydrocarbon extraction. Despite this large number of papers on the topic, very few published studies exist which quantify NMVOC and NO_x emission rates. By far, the majority of emission-based studies have focused on CH_4 which is not so important for air quality. The analysis of these papers highlights large basin-basin variability which causes huge uncertainty in trying to estimate emissions from a new basin. Marrero et al. (2016) provide one of the only alternative studies to those in Uintah cited by Edwards et al. (2014), to evaluate how plausible our emission scenarios could be. Marrero et al. (2016) used whole air samples, collected during October 2013 in the Barnett Shale deposit in northern Texas and found that NMVOC emission rates were greater than 600–1000 kg h^{-1}. Our extra NMVOC emissions range from 88 to 373 kg h^{-1} (per grid box) and so are of similar magnitude to those observed in the Barnett Shale deposit.

NO_2 and O_3 are key pollutants included in the calculation of the Daily Air Quality Index (DAQI) for the UK (Connolly et al. 2013; Neal et al. 2014). Since the emission scenarios considered here only include additional sources for NO_x and NMVOCs which are implemented in AQUM, the main impact will be on the modelled simulation of surface NO_2 and O_3. The impact on the surface concentrations of $PM_{2.5}$ is expected to be minor because the emissions of aerosol precursors in CLASSIC have not been altered. Note, however, that the change in the atmospheric concentrations of oxidants (O_3, OH, HO_2, H_2O_2 and HNO_3) within the RAQ chemistry scheme of AQUM—resulting from the photochemical processing of the additional sources related to fracking—will have an impact on the formation of ammonium sulphate and

Fig. 1 Locations of fracking licences granted in the UK (as of 1 January 2015) and used to constrain the extent and locations for extra emissions (purple polygons). The key areas to note are (i) the Jurassic Weald Basin in the South East of England, (ii) the Carboniferous Bowland-Hodder Shale in the North of England and (iii) the Carboniferous Midland Valley of Scotland. Overlaid are the spatial locations of measurement stations that form the AURN network (black dots)
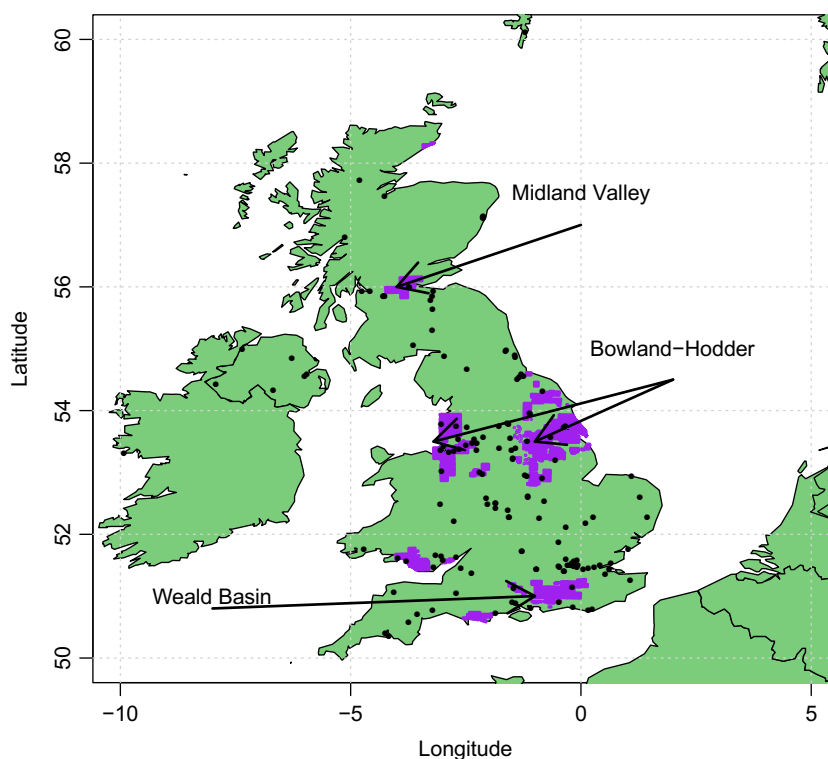
ammonium nitrate in CLASSIC. Therefore, only a lower limit of the effect of fracking emissions on $PM_{2.5}$ can be assessed with the current experimental set-up.

The main focus of our work here is on NO_2 and O_3 and we omit assessing the impacts on $PM_{2.5}$, but note that it is likely that increases in $PM_{2.5}$ emissions (especially from the use of heavy diesel machinery (Hasheminassab et al. 2014)) would have significant health impacts.

Results

Here, we present an analysis of hourly mixing ratios of gas-phase species simulated at the lowest model layer in AQUM. The calculation of the DAQI treats each pollutant with its own average period and concentration threshold levels, derived from health impact studies (Connolly et al. 2013; Neal et al. 2014). Following those indications, the following analysis focuses on the maximum daily 8-h running average ozone (MDA8 O_3) and the maximum daily 1-h average NO_2. Given the lack of changes in emissions of $PM_{2.5}$ and consequently small changes in their abundance, we neglect any further analysis of these species.

Figure 2 shows a comparison of the results from the year 2013 control simulation against observations of NO_2 and O_3 at a selection of rural and suburban locations across the UK (see panels for number of sites included in the analysis). Greater than 80% of all simulated mixing ratios of NO_2 and O_3 in the control simulation are within a factor of two of the observations considering hourly data over the full year. The average correlation coefficients for the comparison of modelled against observed hourly NO_2 and MDA8 O_3 are 0.62 and 0.64, respectively, across all sites over the full year. There is a slight positive bias in modelled MDA8 O_3 (average of the mean normalised bias error (MNBE) over all stations ~ 0.04 ppb) and a negative bias in maximum daily 1-h average NO_2 (average MNBE over all stations ~ -0.28 ppb), but in general, the comparison with the AURN observations gives us good confidence that AQUM performs reasonably well over the period investigated. A more detailed evaluation of AQUM has been documented by Savage et al. (2013) and the inclusion of the temporal and vertical emission scaling (discussed in the 'The AQUM model' section) moderately improves the fit to observations over previous versions of the model (not shown). A more comprehensive evaluation of the performance of the control simulation against surface observations across the UK is given in the online supplementary information.

The impacts of including emissions related to the processes associated with fracking, as explored through scenarios 1–4 (Table 1), are shown in Fig. 3 and Table 2 for O_3 and Fig. 4
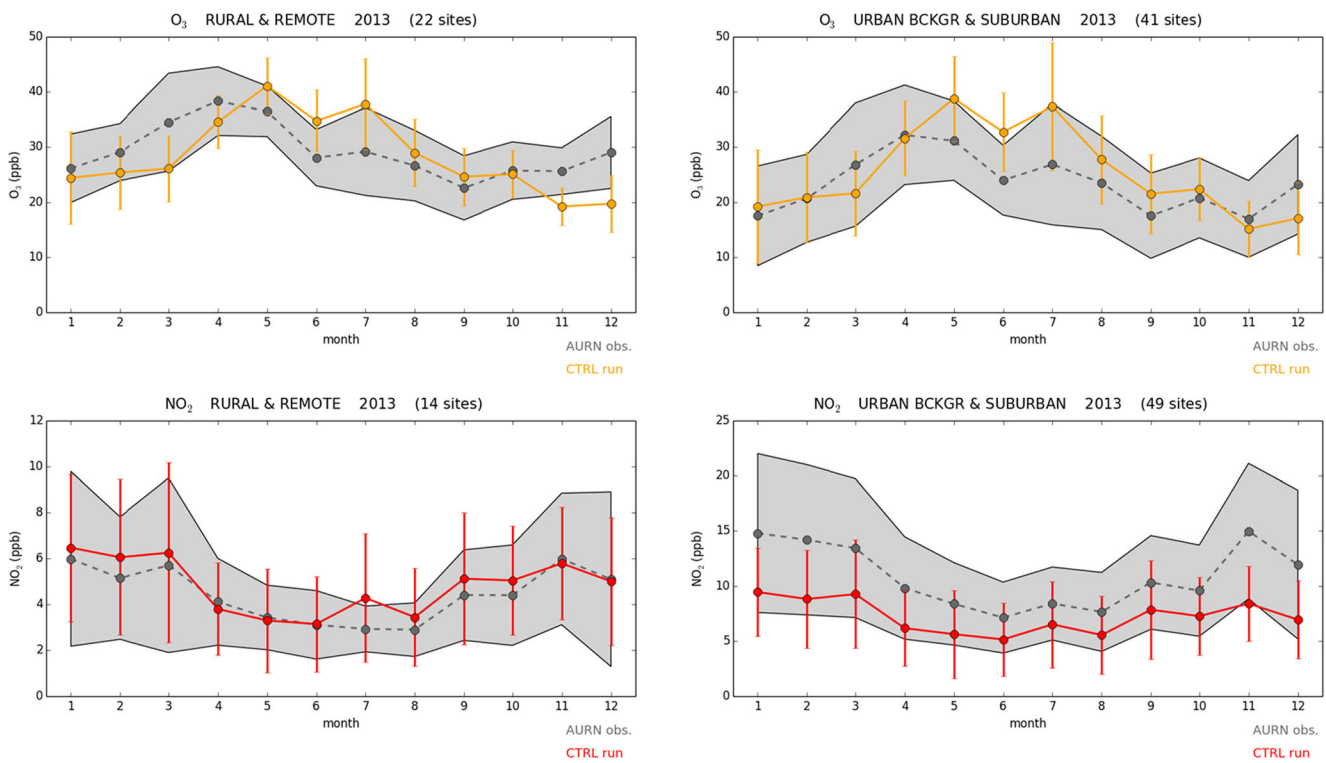

Fig. 2 Comparison of observed (dark grey) and simulated (orange and red from the control run) monthly averaged O_3 and NO_2 mixing ratios across rural and remote and urban background and suburban measurement stations in the AURN network. The shaded areas and vertical bars represent the standard deviations of the hourly observations and the hourly simulated values for each month, respectively
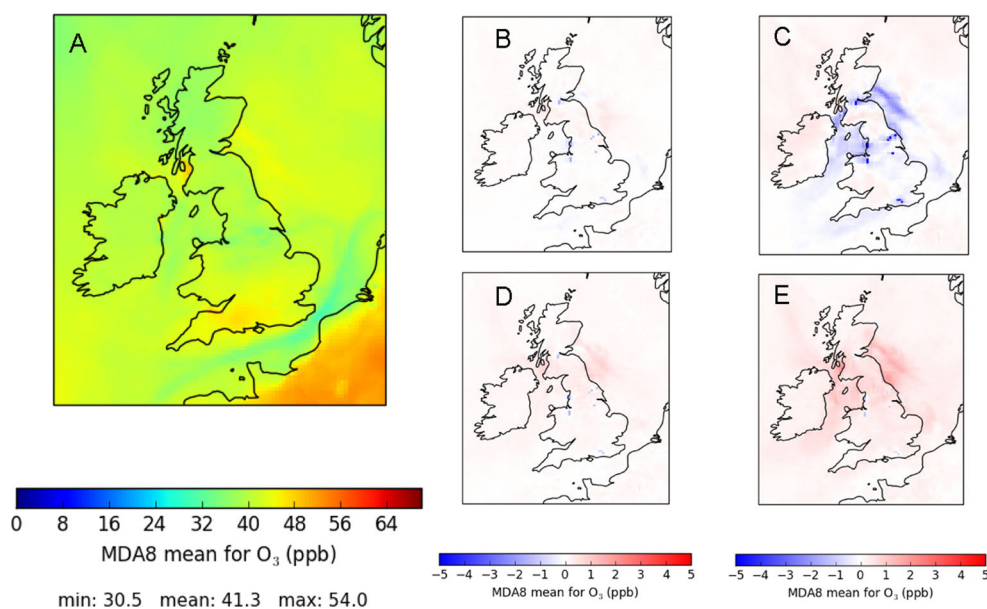
Fig. 3 Monthly mean MDA8 surface O_3 in the control simulation (**a**) and simulated differences for the inclusion of fracking-related activity emissions in scenarios 1–4 (**b–e**) for June 2013. The differences are calculated as scenario X − control simulation. **a** MDA8 O_3 levels simulated by the model for June 2013 are lowest in regions of large shipping activity in the English Channel and generally higher over land—in particular over Northwest France. **b–d** the inclusion of additional VOCs and NO_x emissions in the regions where fracking licences have been granted results in local decreases in O_3 (owing to titration) but varying levels of downwind increases in O_3. The largest increases in O_3 are found for scenario 4 (**e**) where the monthly mean ΔMDA8 O_3 increases by 0.3 ppb on average over the domain shown in the figure

and Table 3 for NO_2. Tables 2 and 3 detail the summary statistics from the analysis for the changes in O_3 and NO_2, respectively, for every month of our simulation for 2013. Table 2 highlights that in general, the largest changes in the area averages for O_3 occur in the summer months (June and July). In Figs. 3 and 4, panel a displays the monthly mean MDA8 O_3 and monthly mean daily 1-h maximum NO_2 for June 2013 in the control simulation, respectively. Whilst the introduction of the fracking-related emissions leads to changes in O_3 and NO_2 year-round (as shown in Tables 2 and 3), photochemical secondary oxidant production is usually greatest in the summer months, hence the focus of our analysis

Table 2 Results for changes in monthly mean daily mean 8-h maximum O_3 mixing ratio (ppb) between control simulation and scenarios for each month in 2013. The results show the area averaged mean change across the study area (avg) (11° W–6° E, 49° N–61° N) as well as the maximum (max) and minimum (min) changes in any grid box. The implementation of large increases in VOC emissions in scenario 3 leads to large maximum increases in O_3 (2.3 ppb in June) and the largest area wide average changes in O_3 (100 ppt on the annual mean)

| Scenario	Jan	Feb	Mar	Apr	May	Jun	Jul	Aug	Sep	Oct	Nov	Dec
1 (min)	− 4.3	− 3.4	− 2.7	− 1.7	− 1.9	− 1.9	−2	− 2.8	− 3.1	− 3.1	− 3.8	−3
1 (avg)	0	0	0	0	0	0.1	0.1	0	0	0	0	0
1 (max)	0.2	0.3	0.3	0.5	0.3	0.8	1	0.5	0.2	0.4	0.6	0.4
2 (min)	− 12.4	−9	− 6.5	− 5.1	−6	− 6.3	− 8.1	− 7.7	− 9.5	−9	− 10.2	−9.9
2 (avg)	− 0.1	− 0.1	− 0.1	− 0.1	− 0.1	0	0.1	− 0.1	− 0.2	− 0.1	− 0.1	−0.1
2 (max)	0.5	0.3	0.4	0.2	0.4	1.6	1.1	0.5	0.2	0.3	1.8	0.8
3 (min)	− 4.3	− 3.3	− 2.6	− 1.6	− 1.8	− 1.7	− 1.7	− 2.6	− 2.8	−3	− 3.7	−3
3 (avg)	0	0	0	0	0	0.1	0.2	0.1	0	0	0	0
3 (max)	0.2	0.3	0.2	0.4	0.5	1.1	1	0.5	0.4	0.3	0.6	0.4
4 (min)	− 4.2	−3	− 2.5	− 1.5	− 1.6	− 1.3	− 1.1	− 2.2	− 2.2	−3	− 3.8	−3
4 (avg)	0	0	0	0	0.1	0.3	0.5	0.2	0.1	0	0	0
4 (max)	0.3	0.4	0.3	0.6	0.9	2.3	2.2	1.1	0.8	0.3	0.6	0.4
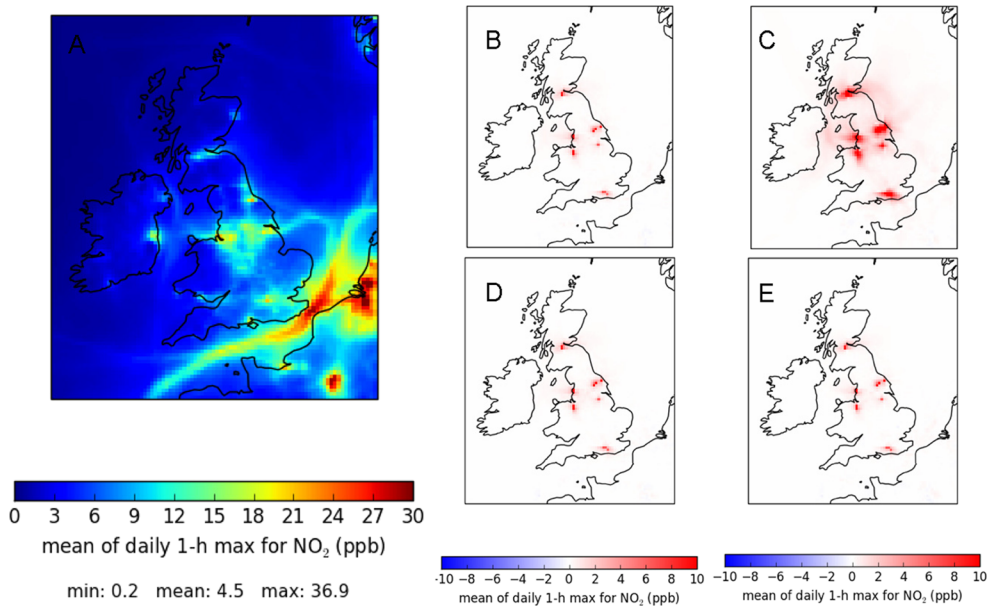
Fig. 4 Monthly mean of the daily 1-h maximum surface NO_2 in the control simulation (**a**) and simulated differences for the inclusion of fracking-related activity emissions in scenarios 1–4 (**b**–**d**) for June 2013. The differences are calculated as scenario X − control simulation. **a** the monthly mean 1-h maximum NO_2 levels simulated by the model for June 2013 are lowest in remote regions, such as the North Sea around Scotland and are highest in regions of large shipping activity in the English Channel and generally high over heavily populated areas of land—in particular, over Benelux. **b**–**d** the inclusion of additional VOC and NO_x emissions in the regions where fracking licences have been granted results in significant local increases in NO_2. The largest increases in NO_2 are found for scenario 2 (**c**) where the monthly mean daily maximum 1-h NO_2 increases by ~ 0.4 ppb on average over the domain shown here and at maximum by ~ 30 ppb

of the June results. We restrict the geographical focus of our work to areas of the UK, as emissions from the UK tend to have negligible impacts on O_3/NO_2 in mainland Europe.

In general, there is a degree of negative correlation in the spatial distribution of O_3 and NO_2—where NO_2 is high, O_3 is low and vice versa. This pattern is well explained through the reaction of NO with O_3, which is a primary mechanism for the production of NO_2 and accounts for a process termed O_3 titration in urban areas. Figure 3a highlights that O_3 titration takes place in the English Channel whereas MDA8 O_3 shows highest levels over suburban areas in Northern France and Southern England. Panels b–e in Fig. 3 show the difference

Table 3 Results for changes in monthly mean 1-h daily mean maximum NO_2 mixing ratio (ppb) between control simulation and scenarios for each month in 2013. The results show the area averaged mean change across the study area (avg) (11° W–6° E, 49° N–61° N) as well as the maximum (max) and minimum (min) changes in any grid box. The implementation of large increases in NO_x emissions in scenario 2 leads to large maximum increases in NO_2 and the largest area wide average changes in NO_2

Scenario	Jan	Feb	Mar	Apr	May	Jun	Jul	Aug	Sep	Oct	Nov	Dec
1 (min)	− 0.3	− 0.3	− 0.3	− 0.4	− 0.6	− 0.4	− 0.4	− 0.5	− 0.3	− 0.4	− 0.3	− 0.4
1 (avg)	0.1	0.1	0.1	0.1	0.1	0.1	0.1	0.1	0.1	0.1	0.1	0.1
1 (max)	4.9	5.8	7.9	9.3	10.2	10.6	16.8	9.9	8.7	7.2	6.2	5.2
2 (min)	− 0.3	− 0.2	− 0.4	− 0.4	− 0.4	− 0.3	− 0.6	− 0.5	− 0.3	−0 .4	− 0.6	− 0.4
2 (avg)	0.4	0.3	0.3	0.3	0.3	0.3	0.3	0.3	0.3	0.3	0.4	0.3
2 (max)	14.4	16	18.1	21.2	25.3	29.7	32.2	24.3	19.3	17.9	13.6	14.2
3 (min)	− 0.3	− 0.4	− 0.4	− 0.4	− 0.5	− 0.5	− 0.4	− 0.6	− 0.5	− 0.4	−0 .4	− 0.4
3 (avg)	0.1	0.1	0.1	0.1	0.1	0.1	0.1	0.1	0.1	0.1	0.1	0.1
3 (max)	4.9	5.9	8	9.3	10.1	10.5	17.1	9.9	8.7	7.3	6.2	5.1
4 (min)	− 0.4	− 0.3	− 0.4	− 0.4	− 0.9	− 0.4	− 0.8	− 0.5	− 0.3	− 0.5	− 0.3	− 0.4
4 (avg)	0.1	0.1	0.1	0.1	0.1	0.1	0.1	0.1	0.1	0.1	0.1	0.1
4 (max)	4.9	6.2	7.9	9.3	10.1	10.5	16.9	9.9	9	7.2	6.3	5.1

in monthly mean MDA8 (ΔMDA8) for June 2013 between the fracking activity scenarios and the control simulation shown in panel a.

Panel b displays ΔMDA8 between scenario 1 and the control simulation. Over the domain, there is an average increase in MDA8 O_3 of 0.1 ppb, but larger local decreases in the regions where fracking activity emissions were included (a maximum decrease of − 1.9 ppb). Panel c highlights that the impacts of scenario 2 are large local decreases in O_3 in the grid squares where emission perturbations are applied (up to − 6 ppb), relatively small decreases in the surrounding cells and a smaller regional increase in O_3 elsewhere (up to 1.5 ppb) which results in effectively no change in the net area averaged ΔMDA8 O_3. Scenario 2 included much larger perturbations to the NO_x and VOC emissions than scenario 1.

Panels d and e display ΔMDA8 O_3 for the differences between scenarios 3–4 and the control, respectively. Scenario 3 includes increased VOC emissions over scenario 1 and comparison of panels b and d highlights that the increased VOC emissions minimise the magnitude of the local ΔMDA8 decreases in the grid cells that contain fracking licences. Panel e shows that further increases in VOC emissions yield slightly higher increases in regional O_3 levels in the model (area weighted ΔMDA8 0.3 ppb), particularly in the outflow regions of the emission perturbations and over the Irish and North Seas, with maximum local increases of 2.3 ppb. Very similar results are found for July (not shown).
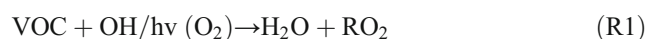
Figure 4 (panel a) illustrates that the maximum NO_2 values simulated by AQUM are present over the dense shipping lanes of the English Channel and large urban centres (cities with population > 400,000 persons). Panel b shows that the difference in monthly mean 1-h mean daily maximum NO_2 (ΔHMDM NO_2) between scenario 1 and the control simulation for June 2013 ranges from 0 to 10 ppb with the largest increases in the model grid cells where the emission perturbations were applied. In panel c, the results from scenario 2 for ΔHMDM NO_2 are presented and demonstrate that with much larger increases in NO_2 emissions, the simulated increases in ΔHMDM NO_2 are of the same order of magnitude. In panel c, the maximum ΔHMDM NO_2 is ∼ 30 ppb (i.e. a factor of 3 increases in ΔHMDM NO_2 for a factor of 4 increases in the additional NO_x emissions from fracking compared to panel b). These increases in ΔHMDM NO_2 are very large compared with the control simulation (panel a). Of particular importance is the fact that the large increases in ΔHMDM NO_2 are spread out over significant distances from the grid cells where the emissions were modified and the emission perturbations therefore impact the levels of HMDM NO_2 in several large urban areas in the UK (particularly in the South East, in places like London; in the North of England, in places like Manchester; and in Scotland, in places like Glasgow and Edinburgh).

Panels d and e compare the results from scenarios 3–4 for ΔHMDM NO_2. These scenarios reflect no difference in NO_x emissions relative to scenario 1 but increases in VOC emissions (by a factor of 2 and 4, respectively, compared to scenario 1). The impacts of increasing VOC emissions on ΔHMDM NO_2 are minimal (< 0.2 ppb).
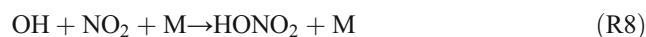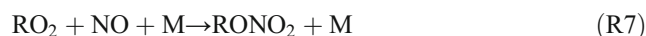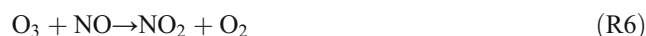
Discussion

In general, the scenarios we have explored with AQUM result in very small impacts on O_3 but significant and large impacts on NO_2. The small impacts on O_3 are surprising given the increases in emissions applied to the precursors (Table 1).

The general chemistry responsible for controlling the production of ozone is discussed in detail by Monks et al. (2015), but briefly revolves around the following cycles of reactions:

$$VOC + OH/hv\ (O_2) \rightarrow H_2O + RO_2 \qquad (R1)$$

$$RO_2 + NO \rightarrow RO + NO_2 \qquad (R2)$$

$$NO_2 + hv \rightarrow O(^3P)\ + NO \qquad (R3)$$

$$O(^3P) + O_2 + M \rightarrow O_3 + M \qquad (R4)$$

$$RO + O_2 \rightarrow HO_2 + OVOC \qquad (R5)$$

where M refers to a third body and RO_2 represent the class of organic peroxy radicals formed from the oxidation of VOCs. With sufficient amounts of NO_x and HO_2/RO_2, the reactions outlined in R1–R5 will tend to produce large amount of O_3. However, as the amount of NO_x increases, the following reactions become important:

$$O_3 + NO \rightarrow NO_2 + O_2 \qquad (R6)$$

$$RO_2 + NO + M \rightarrow RONO_2 + M \qquad (R7)$$

$$OH + NO_2 + M \rightarrow HONO_2 + M \qquad (R8)$$

The first of these reactions (R6) leads to local depletion of O_3 but will lead to subsequent O_3 formation if the products of the reaction (NO_2) go on to photolyse and reproduce O_3 (R3 + R4). However, if the fate of NO_2 is reaction with OH (R8), then there is loss of NO_x from the system as $HONO_2$ represents a very soluble species with a long lifetime and low yield towards releasing NO_x back to the atmosphere. This sequence of reactions (R1–R8) gives rise to the non-linear dependence of ozone to its precursor emissions. The balance between catalytic ozone production (R1–R5) and ozone loss is controlled by the abundance of VOCs and NO_x and the rate constants involved in the elementary reactions. Scenarios 1–4 sample a wide range of VOC and NO_x emissions to investigate this chemistry. Edwards et al. (2014) used a similar approach to understand the controls on O_3 in the Uintah Basin in Utah. Under the conditions observed in Uintah, VOC chemistry was

found to dominate the radical chemistry that propagates O_3 formation and the greatest sensitivity to modelled O_3 was found by modifying NO_x emissions. The results presented in Figs. 3 and 4 demonstrate that in our modelling study, there is a traditional non-linear behaviour in O_3 upon modifying NO_x and VOC emission. A fourfold increase to the additional NO_x emission from fracking (scenarios 2–1) leads to a threefold increase in ΔHMDM NO_2 concentrations, whilst a fourfold increase in VOC emissions from fracking (scenarios 4–1) reduces the change in minimum MDA8 O_3 by 31%.

The fact that the large changes applied to the model emissions of VOC and NO_x (see Table 1) did not give rise to the sorts of increases in O_3 reported in Edwards et al. (2014) is at first confusing but can be rationalised by considering the fact that O_3 chemistry in the Uintah Basin (Edwards et al. 2014) was greatly facilitated by local meteorological conditions in the form of stable shallow boundary layer inversions. The Uintah O_3 pollution events happen often during the winter, when the height of the boundary layer is much shallower than in other seasons and where snow cover can act to increase the short-wave radiation flux required to trigger ozone production (Edwards et al. 2014).

In the UK, these sorts of meteorological conditions do not happen to the same extent. Of particular relevance to our study is the fact that most of the locations we investigated are relatively close to the coast and so would be affected by local scale meteorological mixing in the form of sea/land breezes. It is interesting to consider how changes in meteorology may affect the results from the model. For example, under the conditions favourable for photochemical production that occurred over the UK during several weeks of summer of 2003 (e.g. Lee et al. 2006), we speculate that the impacts on simulated O_3 would be much more severe.

In spite of only small changes to surface O_3 in our model simulations, the potential impacts on air quality from our study are still important to determine. In order to assess the impacts that the changes in NO_2 and O_3 could have on human health, we followed the methodology of Lelieveld et al. (2015) to calculate the impacts on premature mortality as a result of the different scenarios. The change in premature mortality ΔMort can be calculated based on Eq. (1):

$$\Delta\text{Mort} = y_0[1\exp(-\beta\Delta[X])] \times \text{Pop} \qquad (1)$$

y_0 is the UK baseline mortality rate (taken from the WHO http://www.who.int/healthinfo/global_burden_disease/projections/en/). The exponential term reflects the relative risk of a change in pollutant—Δ[X] (calculated from the absolute change in the concentration of pollutant between a given scenario and the control simulation)—and the pollutant-specific concentration response factor (CRF) is given by β. Pop refers to the gridded population density (data taken from

the University of Columbia and NASA SEDAC database http://sedac.ciesin.columbia.edu/).

CRF values for O_3 were taken from a recent study on the Health Risks of Air Pollution in Europe (HRAPIE) (WHO 2013). The HRAPIE study (WHO 2013) recommended CRF values for changes in all-cause mortality associated with changes in annual mean NO_2 of 1.055 (1.031–1.080 range of the 95% confidence interval (CI95)). In our study, we also used 30% lower CRF values for NO_2 to account for the effects of $PM_{2.5}$ highlighted by the HRAPIE study following Walton et al. (2015). We also note that in our calculations, we use CRFs for long-term exposure (as the lifetime of the fracking wells is expected to exceed 5 years). The uncertainty in long-term CRFs is much greater than in short-term CRFs and is an area of vital further work.

To account for the thresholds in exposure to pollutants that health effects have, our calculations of ΔMort include only grid boxes that exceeded annual average NO_2 of 20 μg m^{-3} and seasonal (April–September) average O_3 of 70 μg m^{-3} (following the recommendations of WHO (2013)). Equation (1) was applied for changes in NO_2 and O_3 in each grid box in the model and the resulting ΔMort taken as the sum of the results for each grid box. Our calculation of the total ΔMort is then the sum of the contributions from O_3 and NO_2 taken respectively. In all cases, the ΔMort calculated reflected the difference from the control simulation of the concentration of the pollutant in the scenario under consideration applying the above thresholds on the control and scenario fields. For each of the four scenarios, the calculation of ΔMort was performed
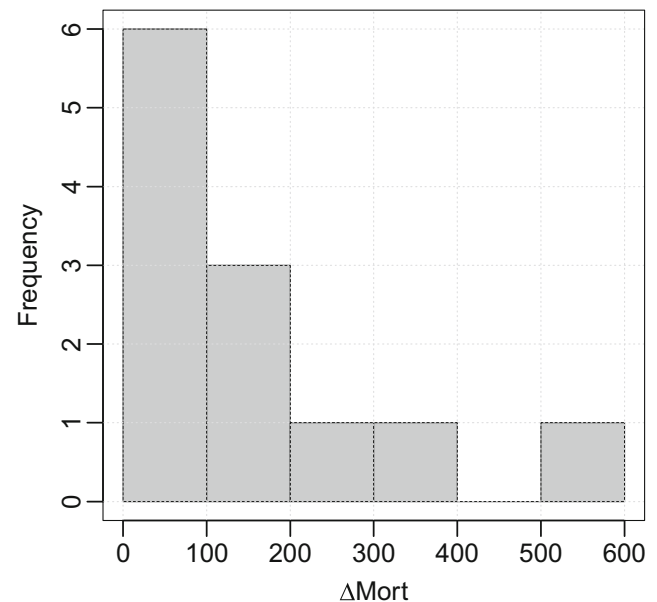

Fig. 5 Histogram of calculated changes in mortality (estimated number of attributable air pollution deaths) following the changes in NO_2 and O_3 modelled in this study for 2013. The changes in mortality reflect the results from the four scenarios calculated under the range of the CI95 values for the CRFs for NO_2 and O_3

using the range of the 95th percentile confidence interval (CI95) values for the CRF values of O_3 and NO_2 yielding a total of 12 estimates of the mortality impacts of fracking-related emissions. Figure 5 shows a histogram of the 12 calculations of ΔMort. The median increase in deaths that was calculated based on the range of scenarios explored is 111 per year across the UK with a range of 51 to 533. Figure 5 shows that the results of our calculations tend to have a very skewed distribution. The changes in mortality as we have calculated them here are all due to changes in NO_2 concentrations with the greatest effects on premature all-cause mortality being attributed to the simulated changes in NO_2 in scenario 2.

The lack of any health effects from the changes in O_3 is owing to both the small number of grid boxes in the model simulations that have seasonal average (April–September) O_3 above 70 μg m^{-3} and the lack of any large increases in O_3 in the scenarios we explored.

Conclusions

In this study, we aimed to assess the potential role that increases in emissions of VOCs and NO_x—important precursors to ground-level ozone—associated with the life cycle emissions related to unconventional hydrocarbon extraction could have on the burden and health effects of air pollutants in the UK.

Following the assumption of minimal emissions of VOCs and NO_x from fracking wells themselves, we derived an emission scenario to explore the impacts of fracking-related emissions based on current emission data for the UK. Present-day model grid-cell maximum emissions from the extraction and distribution of fossil fuels and geothermal energy or road transport were used as a starting point to generate our emission scenario. These extra emissions were included into the AQUM model in the model grid cells where licences for fracking have been granted in three major geological basins—the Weald, the Bowland-Hodder and the Midland Valley.

Further sets of emission scenarios were then generated to allow us to systematically explore the effects of combined and isolated increases in VOCs and NO_x emissions. These emission scenarios were then included into a model simulation for the year 2013 and analysis focused on the impacts of inclusion of the extra emissions relative to a control simulation during June (a peak period for photochemical activity). By far, the biggest impact of the inclusion of the extra fracking emissions was on NO_2—with a monthly mean daily maximum 1-h NO_2 increased by ~0.4 ppb on average over all of the UK and Ireland and large-scale local increases of up to 30 ppb. Much smaller impacts were simulated for O_3, in spite of the large increases in VOC and NO_x emissions.

The effect of the increases in NO_2 and changes in O_3 was assessed by calculating changes in premature mortality following Lelieveld et al. (2015). Considering our emission scenarios, our calculations suggest that the median increase in deaths associated with fracking-related emissions is 111 per year across the UK with a range of 51 to 533.

This study has provided the first assessment of the air quality impacts of the adoption of wide-scale fracking in the UK using a numerical modelling framework. There is undoubtedly large uncertainty as to what the magnitude and distribution of emissions will look like in the future, but the results of this study provide useful evidence for the impacts of poor controls on fracking-related emissions. We conclude that in order to protect air quality and human health, fracking activities must adopt as stringent as possible emission control technology.

References

Adgate J, Goldstein B, McKenzie L (2014) Potential public health hazards exposures and health effects from unconventional natural gas development. Environ Sci Technol 48(15):8307–8320

Andrews IJ 2013 The Carboniferous Bowland Shale gas study: geology and resource estimation British Geological Survey for Department of Energy and Climate Change London UK

Andrews IJ 2014 The Jurassic shales of the Weald Basin: geology and shale oil and shale gas resource estimation British Geological Survey for Department of Energy and Climate Change London UK

Bickle M (2012) Shale gas extraction in the UK: a review of hydraulic fracturing The Royal Society and The Royal Academy of Engineering: London UK; https://royalsociety.org/~/media/policy/projects/shale-gas-xtraction/2012-06-28-shale-gas.pdf

Bieser J, Aulinger A, Matthias V, Quante M, Denier van der Gon HAC (2011) Vertical emission profiles for Europe based on plume rise calculations. Environ Pollut 159:2935–2946

BP 2014 BP Energy Outlook 2035 available at: bpcom/energyoutlook (last access: 4 August 2015)

Brunekreef B, Holgate S (2002) Air pollution and health. Lancet 360(9341):1233–1242

Connolly E et al 2013 Update on implementation of the Daily Air Quality Index: information for data providers and publishers Defra Report available at http://uk-air.defra.gov.uk/reports/cat14/1304251155_Update_on_Implementation_of_the_DAQI_April_2013_Final.pdf (last access: 17 June 2016)

Denier van der Gon H et al 2011 Description of current temporal emission patterns and sensitivity of predicted AQ for temporal emission patterns EU FP7 MACC deliverable report D_D-EMIS_13 TNO report

available at http://gmes-atmosphere.eu/documents/deliverables/d-emis/MACC_TNO_del_1_3_v2.pdf (last access: 17 June 2016)

Edwards PM, Brown SS, Roberts JM, Ahmadov R, Banta RM, deGouw JA, Dubé WP, Field RA, Flynn JH, Gilman JB, Graus M, Helmig D, Koss A, Langford AO, Lefer BL, Lerner BM, Li R, Li SM, McKeen SA, Murphy SM, Parrish DD, Senff CJ, Soltis J, Stutz J, Sweeney C, Thompson CR, Trainer MK, Tsai C, Veres PR, Washenfelder RA, Warneke C, Wild RJ, Young CJ, Yuan B, Zamora R (2014) High winter ozone pollution from carbonyl photolysis in an oil and gas basin. Nature 514(7522):351–354

Environmental Audit Committee 2015 Eighth report of session 2014–15 environmental risks of fracking HC 856 (last access: 17 June 2016)

Flemming J, Inness A, Flentje H, Huijnen V, Moinat P, Schultz MG, Stein O (2009) Coupling global chemistry transport models to ECMWF's integrated forecast system. Geosci Model Dev 2:253–265

Hasheminassab S, Daher N, Ostro BD, Sioutas C (2014) Long-term source apportionment of ambient fine particulate matter (PM_{25}) in the Los Angeles Basin: a focus on emissions reduction from vehicular sources. Environ Pollut 193:54–64

International Agency for Research on Cancer 2012 IARC: diesel engine exhaust carcinogenic https://www.iarcfr/en/media-centre/pr/2012/pdfs/pr213_E.pdf (last access: 17 June 2016)

Kuenen J et al (2014) TNO-MACC_II emission inventory; a multi-year (2003–2009) consistent high-resolution European emission inventory for air quality modelling. Atmos Chem Phys 14:10963–10976

Lee J et al (2006) Ozone photochemistry and elevated isoprene during the UK heatwave of August 2003. Atmos Environ 40:7598–7613

Lelieveld J, Evans JS, Fnais M, Giannadaki D, Pozzer A (2015) The contribution of outdoor air pollution sources to premature mortality on a global scale. Nature 525(7569):367–371

Mailler S, Khvorostyanov D, Menut L (2013) Impact of the vertical emission profiles on background gas-phase pollution simulated from the EMEP emissions over Europe. Atmos Chem Phys 13:5987–5998

Marrero JE, Townsend-Small A, Lyon DR, Tsai TR, Meinardi S, Blake DR (2016) Estimating emissions of toxic hydrocarbons from natural gas production sites in the Barnett Shale region of Northern Texas. Environmental science & technology 50:10756–10764

Monaghan AA (2014) The carboniferous shales of the Midland Valley of Scotland: geology and resource estimation British Geological Survey for Department of Energy and Climate Change London UK

Monks PS, Archibald AT, Colette A, Cooper O, Coyle M, Derwent R, Fowler D, Granier C, Law KS, Mills GE, Stevenson DS, Tarasova O, Thouret V, von Schneidemesser E, Sommariva R, Wild O, Williams ML (2015) Tropospheric ozone and its precursors from the urban to the global scale from air quality to short-lived climate forcer. Atmos Chem Phys 15(15):8889–8973

Moore C et al (2014) Air impacts of increased natural gas acquisition processing and use: a critical review. Environ Sci & Tech 48(15):8349–8359

Neal LS, Agnew P, Moseley S, Ordóñez C, Savage NH, Tilbee M (2014) Application of a statistical post-processing technique to a gridded operational air quality forecast. Atmos Environ 98:385–393

Passant N et al 2014 UK Informative Inventory Report (1980 to 2012) available at http://uk-air.defra.gov.uk/assets/documents/reports/cat19/1405130812_UK_IIR_2014_Final.pdf (last access: 17 June 2016)

Savage NH, Agnew P, Davis LS, Ordóñez C, Thorpe R, Johnson CE, O'Connor FM, Dalvi M (2013) Air quality modelling using the Met Office Unified Model (AQUM OS24 26): model description and initial evaluation. Geosci Model Dev 6:353–372

Sillman S (1999) The relation between ozone, NOx and hydrocarbons in urban and polluted rural environments. Atmos Environ 33:1821–1845

Simpson D, Benedictow A, Berge H, Bergström R, Emberson LD, Fagerli H, Flechard CR, Hayman GD, Gauss M, Jonson JE, Jenkin ME, Nyíri A, Richter C, Semeena VS, Tsyro S, Tuovinen JP, Valdebenito Á, Wind P (2012) The EMEP MSC-W chemical transport model - technical description. Atmos Chem Phys 12:7825–7865

Sommariva R, Blake RS, Cuss RJ, Cordell RL, Harrington JF, White IR, Monks PS (2014) Observations of the release of non-methane hydrocarbons from fractured shale. Environ Sci & Tech 48(15):8891–8896

US Energy Information Administration (2015) Assumptions to the Annual Energy Outlook 2015 DOE/EIA-0554 1–154 (last access: 17 June 2016)

Walton H et al 2015 Understanding the health impacts of air pollution in London transport for London and the Greater London Authority

Whall C et al 2010 UK Ship Emissions Inventory Entec UK Ltd London UK available at: http://uk-air.defra.gov.uk/reports/cat15/1012131459_21897_Final_Report_291110.pdf (last access: 17 June 2016) 2010

WHO 2013 Health risks of air pollution in Europe–HRAPIE project Copenhagen: World Health Organization

Vengosh A, Mitch WA, McKenzie LM (2017) Environmental and human impacts of unconventional energy development. Environ Sci Technol 51:10271–10273